HHS Public Access

Author manuscript

Lancet Neurol. Author manuscript; available in PMC 2017 January 01.

Published in final edited form as:

Lancet Neurol. 2016 January ; 15(1): 56–64. doi:10.1016/S1474-4422(15)00323-3.

Rates of transition between amyloid and neurodegeneration biomarker states and to dementia among non-demented individuals: a population-based cohort study

Clifford R. Jack Jr., M.D.[a], **Terry M. Therneau, Ph.D.**[b], **Heather J. Wiste, B.A.**[b], **Stephen D. Weigand, M.S.**[b], **David S. Knopman, M.D.**[c], **Val J. Lowe, M.D.**[a], **Michelle M. Mielke, Ph.D.**[b], **Prashanthi Vemuri, Ph.D.**[a], **Rosebud O. Roberts, M.D.**[b], **Mary M. Machulda, Ph.D.**[d], **Matthew L. Senjem, M.S.**[a], **Jeffrey L. Gunter, Ph.D.**[a], **Walter A. Rocca, M.D., M.P.H.**[b], and **Ronald C. Petersen, Ph.D., M.D.**[c]

[a]Department of Radiology, Mayo Clinic and Foundation, 200 First Street SW, Rochester, MN 55905, USA

[b]Department of Health Sciences Research, Mayo Clinic and Foundation, 200 First Street SW, Rochester, MN 55905, USA

[c]Department of Neurology, Mayo Clinic and Foundation, 200 First Street SW, Rochester, MN 55905, USA

[d]Department of Psychiatry and Psychology, Mayo Clinic and Foundation, 200 First Street SW, Rochester, MN 55905, USA

Summary

Background—We previously observed in a cross-sectional analysis that frequencies of amyloid and neurodegeneration biomarker states varied greatly by age among cognitively non-impaired participants, suggesting dynamic within-person processes. Our objective in this longitudinal study was to estimate rates of transitioning from a less- to a more-abnormal biomarker state by age among non-demented individuals, as well as rates of transitioning to dementia by biomarker state.

Methods—All participants (n=4049) were non-demented at baseline. A subset of 1541 underwent multi-modality imaging. Amyloid PET was used to classify individuals as amyloid positive (A+) or negative (A−). FDG PET and MRI were used to classify individuals as neurodegeneration positive (N+) or negative (N−). All observations from the 4049 individuals were used in a multi-state model to estimate four different age-specific biomarker state transition rates among non-demented individuals: A−N− to A+N−; A−N− to A−N+ (suspected non-Alzheimer pathology, SNAP); A+N− to A+N+; A−N+ (SNAP) to A+N+. We also estimated two

Corresponding Author: Clifford R. Jack, Jr., M.D., Department of Radiology, 200 First Street SW, Rochester, MN 55905, 507 293-3793 (phone), 507 284-9778 (fax), jack.clifford@mayo.edu.

age-specific rates to dementia: A+N+ to dementia; and A−N+ (SNAP) to dementia. Using these state-to-state transition rates, we estimated biomarker state frequencies by age.

Findings—All transition rates were low at age 50 and (with one exception) were well-characterized by an exponential increase with age. The rates per 100-person years at ages 65 versus 85 were 1.6 versus 17.2 for A−N− to A−N+, 6.1 versus 20.8 for A+N− to A+N+, 2.6 versus 13.2 for A−N+ to A+N+, 0.8 versus 7.0 for A+N+ to dementia, and 0.6 versus 1.7 for A−N+ to dementia. The one exception to an exponential increase with age was the transition rate from A−N− to A+N− which increased from 4.0 transitions per 100 person-years at age 65 to approximately 7 transitions per 100 person-years in the 70s and then plateaued beyond that age. Estimated biomarker frequencies by age from the multistate model were similar to cross-sectional biomarker frequencies.

Interpretation—Dynamic state-to-state transition rates illustrate important measurable aspects of the changing biology underlying brain aging. The biomarker states we describe relate to both AD and non-AD processes. Our transition rates suggest that brain aging can be conceptualized as a nearly inevitable *acceleration* toward worse biomarker and clinical states. The one exception was that transition to amyloidosis without neurodegeneration was most dynamic from age 60 to 70 and then plateaued beyond that age. We found that simple transition rates can explain complex, highly interdependent biomarker state frequencies in our sample.

Keywords

Cognitive aging; Brain aging; Amyloid imaging; Alzheimer disease; Brain atrophy and Alzheimer disease; FDG PET and Alzheimer disease

Introduction

Current recommendations for use of biomarkers in research diagnostic criteria for Alzheimer's disease (AD) require that individuals are categorized as either normal or abnormal on biomarkers of amyloidosis and neurodegeneration.[1–4] Established biomarkers of amyloidosis are amyloid PET and CSF Aβ42, and established biomarkers of neurodegeneration are CSF tau, FDG PET, and structural MRI. Tau PET imaging will be an important addition.[5, 6] If biomarkers are used to classify individuals as amyloid positive (A+) or negative (A−), and neurodegeneration positive (N+) or negative (N−), then all participants can be placed into one of four biomarker states: A−N−, A+N−, A−N+, or A+N+.

While the A/N biomarker classification system arose from the integration of biomarkers into AD diagnostic criteria,[1–4] the system extends beyond the AD spectrum. Participants who are A−N− have no biomarker evidence of AD pathology. In addition, we have labeled amyloid negative participants who have AD-like neurodegenerative biomarkers (i.e., A−N+) as suspected non-Alzheimer's pathophysiology (SNAP).[7]

In a large sample of cognitively normal for age (not including mild cognitive impairment, MCI) participants aged 50–89 years, from a population-based cohort, we recently observed that frequencies of the four biomarker states (defined by imaging) varied dramatically by age.[8] We hypothesized that the age-dependent variation may be due to transitions of

individual participants from a less- to more-abnormal biomarker state with advancing age. However, because our analysis was cross-sectional, we could not make inferences about rates of transitions between biomarker states.

Transition rates illustrate important measurable aspects of the biology underlying brain aging including both AD and non-AD processes and thus are of interest to a general neurological audience. Our primary objective in this study was to estimate the transition rates between the six states shown in Fig 1: the four non-demented biomarker states of A−N−, A+N−, A−N+ (SNAP), and A+N+ along with transition rates to dementia and death, two states that are fundamental components of any population progression model. The arrows between the boxes (Fig 1) illustrate the possible biological transitions. To estimate these rates, we used a population-based sample of Olmsted County, Minnesota residents who were not demented (i.e., categorized as cognitively normal for age or MCI) at baseline.[9]

Methods

Study design and participants

All participants were enrolled in the Mayo Clinic Study of Aging (MCSA). The MCSA is a longitudinal population-based study of cognitive aging among Olmsted County, Minnesota, residents.[9] Baseline and follow-up MCSA visits occurred approximately every 15 months and included: a medical and history review and an interview with a study partner performed by a study coordinator; a medical history review, mental status examination, and a neurological examination by a physician; and a comprehensive neuropsychological examination [9]. At a consensus conference, the study coordinator, physician, and neuropsychologists determine a clinical diagnosis. For the purposes of this study, participants were assigned a diagnosis of demented or not demented using established criteria for dementia.[3] All 4049 participants in the current study were non-demented at baseline.

Imaging data from the 1541 MCSA participants who had amyloid PET, FDG PET, and MRI scans using identical PET and MRI study protocols were used in the study. The imaging tests were obtained from March 2006 to April 2015. The median time between MRI and PET imaging was: 12 days, interquartile range (IQR): 3–28 days.

This study was approved by the Mayo Clinic and Olmsted Medical Center Institutional Review Boards (both Rochester, MN, USA), and all participants provided written informed consent at the time of enrollment.

Procedures

Amyloid PET imaging was performed with Pittsburgh Compound B.[10] FDG PET was obtained on the same day. Amyloid PET and FDG PET were analyzed with our in-house fully automated image processing pipeline[11] where image voxel values are extracted from automatically labeled regions of interest (ROIs) propagated from an MRI template.

MRI was performed on one of three 3T General Electric systems. The cortical surface was parcellated using Freesurfer (version 5.3). We formed an AD-signature cortical thickness

measure[12] composed of the following individual cortical thickness ROIs: entorhinal, inferior temporal, middle temporal, and fusiform [13]. We used this AD signature thickness measure in the current analysis rather than the more common adjusted hippocampal volume. Unlike hippocampal volume [14], the AD signature thickness measure is not significantly associated with head size and therefore no statistical adjustment for head size is necessary. In addition since men on average have larger heads than women, a gender-dependent head size effect is imparted to hippocampal volume but not to AD signature thickness [15]. We recently demonstrated that important features associated with grouping individuals into amyloidosis and neurodegeneration states are preserved across different imaging definitions of neurodegeneration [13].

Definition of abnormality and biomarker states

The normal/abnormal cut-point for the PET and MRI measures was set at the 90th percentile (mild end of the range) of an updated group of 75 AD patients from the Mayo Clinic using the approach described elsewhere.[7] Abnormal amyloid PET was defined as SUVR >1.40. This cut-point of 1.4 for Pittsburgh Compound B SUVR using our processing pipeline corresponds to Thal phase 1 [16] and therefore our amyloid PET cut-point was supported by the best possible gold standard (autopsy). We used the same criteria for FDG and MRI (90th percentile of ADs) as we did for defining the amyloid PET cut-point. Abnormal FDG PET SUVR was defined as <1.32 and abnormal AD signature cortical thickness as <2.74 mm. Neurodegeneration was defined as abnormal AD signature thickness [13], abnormal FDG PET, or both.

Statistical methods

We used a multi-state Markov (MSM) model to estimate the rates of transition between the different states illustrated in Fig 1. The transition rates of interest in our model were across four biomarker states (A−N−, A+N−, A−N+, or A+N+) among non-demented participants and from the two N+ biomarker states to dementia (see arrows in Fig 1). The model also included rates from each of these states to death and a rate from more abnormal to less abnormal biomarker states (i.e. “backward” transitions) to account for misclassification.

The overall likelihood was maximized using the R statistical package. Our approach closely followed that of the msm package in R.[17] a complete summary is given in the supplementary material. An important feature of our approach is that we took advantage of three types of data. First, because the MCSA is population-based, the initial state of each imaged subject can be viewed as reflective of non-demented subjects of that age and sex. These initial biomarker state frequencies provide one portion of the likelihood to be maximized. Second, subjects with multiple determinations of their state (clinical or imaging) can be compared to computed transition probabilities, providing a second portion of the likelihood. Third, we took advantage of the fact that Olmsted County death rates are nearly identical to those for Minnesota[18]. These rates are almost perfectly log-linear for ages 50–95. We assumed the same slopes and male:female rate ratios for our data set, replacing eight somewhat poorly determined parameters (male and female, intercept and slope, demented, and non-demented) with two parameters, the relative death rate for demented and non-demented as compared to the underlying population.

The MCSA participants who had only a single non-imaging baseline visit and no other follow-up did not contribute any information towards estimating transition rates, and were therefore excluded. All 4049 remaining eligible participants of the MCSA and all visits (clinical or imaging) for those participants were used in the analysis, although the statistical information from each observation varied (see supplementary materials for full details).

Over the age of 50, population death rates are almost perfectly log-linear. Motivated by this we initially modeled all six transition rates of interest, as well as the rates to death, as having the form rate(age) = $\exp(\beta_0 + \beta_1 \text{age})$ where β_0 and β_1 were coefficients to be estimated. Rates of this form are log-linear, i.e., linear after a natural logarithm transformation. We then used likelihood ratio tests to determine whether relaxing the log-linearity assumptions via restricted cubic splines (one rate at a time) improved the model fit. The A−N− to A+N− transition was found to be non-linear (on the log scale); however, no additional non-linear rates further improved the fit.

Other summaries, e.g., population frequencies, can be computed from the fitted rates using standard methods. Assuming for instance a starting cohort of 50-year-old non-demented participants, the predicted population structure at ages 50–90 can be derived. These probabilities can be interpreted as the frequencies of each of the six states (non-demented A −N−, A+N−, A−N+, A+N+; dementia; death) at a given age. We note that because of differences in death rates for men and women, 1-year transition probabilities differ by sex and thus the biomarker frequencies do as well. Therefore, the reported frequency curves are averaged among men and women. We compared these estimated frequencies with those from a cross-section multinomial model to evaluate whether the rates-based model adequately captured the age-related variation in cross-sectional frequencies.

Role of the funding source

The funders of the study had no role in study design, data collection, data analysis, data interpretation, or writing of the report. All authors had full access to all the data in the study. The corresponding author had final responsibility for the decision to submit for publication.

Results

Demographics

A total of 4049 MCSA participants who were non-demented at baseline (3512 [87%] cognitively normal for age and 537 [13%] MCI) were included in our analysis with a subset of 1541 participants undergoing imaging (Table). There were a total of 15,225 clinical assessments, 2193 of which included concurrent imaging assessments (each composed of MRI, FDG PET, and amyloid PET). Among participants with clinical follow-up, there was a median (IQR) of 4.0 (2.1, 7.0) years of follow-up. Among the participants with imaging, 1052 participants had only one imaging assessment, 348 had exactly two, 120 had exactly three, and 21 had more than three. Among the 489 subjects with serial imaging, there was a median (IQR) of 2.6 (1.6, 3.9) years of imaging follow-up.

The proportion of APOE ε4 carriers was greater in participants with amyloidosis (109/247 [44%] in A+N− and 119/283 [42%] in A+N+) than without amyloidosis (157/778 [21%] in

A−N− and 43/233 [19%] in A−N+). Men tended to have more neurodegeneration than women as evidenced by the proportion of men being 9 percentage points higher for A−N+ compared to A−N− (145/233 [62%] vs. 409/778 [53%]) and for A+N+ compared to A+N− (154/283 [54%] vs. 111/247 [45%]).

Annual state-to-state transition rates by age

A table of transitions observed in our data can be found in the supplementary materials. Estimated transition rates corresponding to the arrows in Fig 1 are plotted on the arithmetic scale by age in Fig 2 and separately with 95% CIs on the natural logarithm scale in Fig 3. All transition rates were low at age 50 (fewer than three transitions per 100 person-years for all) and (with one exception) were well-characterized by an exponential increase with age. The one exception was the transition rate from A−N− to A+N− which increased to seven transitions per 100 person-years in the 70s and then plateaued. Overall the confidence bands around the rate estimates were fairly narrow; however, uncertainty in the transition rate estimates was greater at the younger ages, and there was limited precision in the estimate of the A−N+ to dementia rate (Fig 3).

In Figure 4 we present pairwise comparisons of transition rates. We report the estimated difference in transition rate by age along with 95% CIs for the difference. Ages at which the 95% CI does not include zero are interpreted as indicating significant difference in transition rates at $p<0.05$.

The six transition rates are shown in the context of our overall transition model at ages 65, 75 and 85 years in Fig 5. To facilitate comparisons, we point out three different comparison-pairs of transitions moving from left to right (less- to more-abnormal) in the overall model (Fig 1). First, from age 65 to age 85 the A−N− to A+N− rate increased from 4.0 to 7.0 per 100 person-years for a 1.7-fold (95% CI: 0.9–3.6) increase, whereas the A−N− to A−N+ rate increased from 1.6 to 17.2 per 100 person-years for an 11.0-fold (95% CI: 7.4–16.3) increase. Second, the A+N− to A+N+ rate increased from 6.1 to 20.8 per 100 person-years for a 3.4-fold (95% CI: 2.0–5.6) increase, whereas the A−N+ to A+N+ rate increased from 2.6 to 13.2 per 100 person-years for a 5.0-fold (95% CI: 2.1–12.4) increase. Third, the A+N+ to dementia rate increased from 0.8 to 7.0 per 100 person-years for an 8.6-fold (95% CI: 4.7–15.5) increase, whereas the A−N+ to dementia rate increased from 0.6 to 1.7 per 100 person-years for a 2.6-fold (95% CI: 0.2–30.6) increase.

Of secondary interest, the non-demented subjects had a death rate which was 0.53 (95% CI: 0.48, 0.58) times that for an age- and sex-matched sample from the population, while demented subjects' death rate was 2.7-fold (95% CI: 2.4, 3.1). The estimated rate of transitioning from a more-abnormal to a less-abnormal biomarker state (i.e. "backward transitions"), included in the model to account for possible misclassifications, was very low at 0.025. We did not include transitions from A−N− or A+N− to dementia in our model due to the rarity of observed transitions between these states in our data (0 transitions from A+N− to dementia and 1 from A−N− to dementia). Also, we only observed one direct transition from A−N− to A+N+ at the next visit. Instead of directly estimating this rate, our model assumes this subject passed through an intermediate state at some point during the

observation interval. This seems a reasonable assumption as the odds that a transition from A− to A+ and N− to N+ actually occurs at precisely the same instant is infinitesimally small.

Frequencies of six possible states by age

Assuming a cohort of A−N− individuals aged 50, we used the rates from the transition model to estimate the frequency of each state as the cohort ages from 50 to 90 (Fig 6a). The estimated frequency of non-demented individuals (the sum of the frequencies of all four A/N states) decreased dramatically at older ages, with a steeper downward slope from age 70 onward (Fig 6a). The frequency of demented individuals increased beginning in the mid-70s to a maximum of about 7% in the late-80s. The frequency of death increased approximately exponentially reaching 73% by age 90.

Fig 6b illustrates the biomarker state frequency data among those who were non-demented and alive by age so that the frequencies of the four biomarker states sum to 100% at each age. Among those who were alive and non-demented, the frequency of A−N− decreased to 7% by age 90, the frequency of A+N+ increased to 58% by age 90, the frequency of A−N+ increased to a plateau around 24% in the mid-80s, and the frequency of A+N− decreased to 12% at age 90 after peaking at 25% in the 70s.

Fig S1 shows that our multi-state model for the rates captures the observed cross-sectional frequencies quite well and thus provides some validation in support of our fitted model. A simple rate model is useful for describing the underlying change in biology even though the observed states in the population has a much more complex appearance with different states waxing and waning in their contribution by age.

Discussion

Our major findings are: (1) a very simple model for the rates of biomarker transitions can lead to a complex interplay of observed biomarker states. This is important because unlike age-specific frequencies, state-to-state transition rates can be thought of as direct measures of underlying biological processes; (2) incident amyloidosis rates on a background of no preexisting neurodegeneration (A−N− to A+N−) are most dynamic in the 60–75 age range while incident neurodegeneration rates on a background of no preexisting amyloidosis (A−N− to A−N+) are particularly dynamic from about age 70 onward; (3) from about age 70 onward, the rate of developing neurodegeneration after amyloidosis is higher than the rate of developing amyloidosis after neurodegeneration; (4) the transition to dementia almost always requires neurodegeneration, and (5) among those with neurodegeneration, from the late 70s onward the rate of transitioning to dementia is higher among those with amyloidosis than those without.

Comparison of the A−N− to A+N− rate (the light blue line in Fig 2) and the A−N− to A−N+ rate (the light green line in Fig 2) provides insight into the two types of transitions out of A−N−. These are the left-most pair of rates in Figs 1 and 5. The rate of A−N− to A+N− is greater than the rate of A−N− to A−N+ in the 60–75 age range, but in the 80s the rate of A−N− to A−N+ is much higher (Fig 4). This suggests that incident amyloidosis on a background of no preexisting neurodegeneration (A−N− to A+N−) is more characteristic of

non-demented individuals in the 60–75 age range whereas incident neurodegeneration on a background of no preexisting amyloidosis (A−N− to A−N+) is more characteristic of non-demented individuals in their 80s. A+N− identifies someone as being in the AD pathway.[4] In contrast, we[7, 19] have argued that the neurodegeneration in A−N+ (SNAP) participants must represent some mixture of amyloid-independent neurodegenerative or cerebrovascular etiologies that increase in prevalence with aging,[20–22] including aging itself.[23, 24]

The A−N− to A+N− transition deserves special mention because it is the only rate that does not increase exponentially with age. While we cannot definitely say why the A−N− to A+N− rate plateaus in the 70s, we are confident this finding is accurate because the narrow confidence intervals in the top left panel of Fig 3 rule out a straight-line (log-linear) fit. One possible, though speculative, explanation for this plateauing is that the A−N− state consists of two pools of individuals; those who are inherently susceptible to developing amyloidosis and those who are resistant. If this is the case, the rapidly increasing rate of A−N− to A+N− seen from 60–70 would be driven by susceptible individuals who leave the A−N− risk pool upon transition to A+N−. The flat rate in the 70s and beyond would be driven by individuals who are inherently resistant to amyloidosis.

Comparison of the A+N− to A+N+ rate (the dark green line in Fig 2) and the A−N+ to A+N+ rate (the dark blue line in Fig 2) highlights the two pathways into the most advanced biomarker state (A+N+). These are the middle pair of rates in Figs 1 and 5. An A+N− to A+N+ transition denotes an amyloid-first sequence while A−N+ to A+N+ denotes a neurodegeneration-first sequence into A+N+. Throughout the entire age range, the A+N− to A+N+ rate exceeds the A−N+ to A+N+ rate (although the difference is significant only from age 70 to mid-80s), which suggests that the intensity of the amyloid-first pathway is greater throughout adult life.

Comparison of the A+N+ to dementia rate (the dark red line in Fig 2) and the A−N+ (SNAP) to dementia rate (the light red line in Fig 2) provides insight into events leading to dementia. These are the right-most pair of rates in Figs 1 and 5. All participants who transition from A+N+ to dementia would meet International Working Group (IWG) and National Institute of Aging-Alzheimer's Association (NIA-AA) (highest probability) criteria for AD dementia.[1, 3] The A+N+ to dementia rate is greater than the A−N+ (SNAP) to dementia from the late-70s onward (Fig 4), indicting the clinically malignant nature of the A+N+ state.

We have not modeled transitions from A−N− or A+N− directly to dementia because the number of participants in our sample making these direct transitions was negligible and just as importantly, was not necessary to achieve good prediction. The clear implication is that neurodegeneration is the direct temporal precursor to dementia – not isolated amyloidosis (A+N) nor A−N−. This in turn supports the concept that, for individuals in the AD pathway, amyloidosis is necessary but not sufficient to produce AD dementia.[25–30] We did not distinguish between types of dementia in our model. Of the 247 cases of incident dementia, the clinical diagnosis was AD dementia in 166; vascular dementia in 15; and dementia with Lewy bodies in 10. Diagnoses in the remaining cases were less frequent conditions or were simply labeled dementia without a specific hypothesized etiology.

Comparison of the A+N− to A+N+ rate (the dark green line in Fig 2) and the A−N− to A−N+ rate (the light green line in Fig 2) addresses the question, “does amyloid induce neurodegeneration?” The A+N− to A+N+ rate exceeds the A−N− to A−N+ rate from age 50 until the 80’s where the two rates become similar. These data are consistent either with the concept that amyloidosis induces neurodegeneration or that there is a common upstream cause for both throughout much of the adult lifespan.[31, 32]

A motivation for the present study, hypothesized in our 2014 paper [8], was to assess if state-to-state transition rates could explain observed differences in biomarker state frequencies with age. In the current study, which includes all 985 subjects from the 2014 paper, we found that a multi-state model with simple rate functions (all log-linear except one) fit the data well (Fig S1) and thus is useful in explaining complex, highly interdependent state frequencies. The interrelationship between rates and population frequencies is not always intuitive and it is important to understand the distinction between rates and frequencies; the two can be very different. The rates can be thought of as describing the effect of an underlying disease process while the frequencies indicate the number of people in each state observed in the population. The rate of a transition could be very high, but if there are very few people at risk for that transition, the actual number of transitions observed would be small. A commonly used example is the fact that annual death rate among centenarians is very high while the number of observed deaths is small.

In our study, we saw the A+N− to A+N+ rate (a later transition) was always higher than the A−N− to A+N− rate (an earlier transition). This finding would seem unintuitive given that a risk pool of A+N− subjects must exist to undergo transitions to A+N+. However, since the pool of A−N− subjects is much larger than the pool of A+N− subjects at younger ages, the actual number of people transitioning from A−N− to A+N− is larger than the number transitioning from A+N− to A+N+. A key strength of our study is that we can characterize the intensity of different aspects of brain aging via rates and summarize the results of these processes at the population level via frequencies.

Our study has some limitations. With respect to the model fit itself, the clinical follow-up period was relatively short (median 4.0 years, IQR 2.1–7.0) as was the imaging follow-up (median 2.6 years, IQR 1.6–3.9). The study would have been improved by the addition of CSF biomarkers and tau PET. We had inadequate power to analyze the effects of sex and APOE on biomarker transition rates. Thus, APOE ε4 carriers and non-carriers, and men and women were pooled. At the baseline imaging visit; however, those with amyloidosis (both A+N− and A+N+) were more often APOE carriers (Table), and a higher proportion of men than women were neurodegeneration positive. Thus, we do see sex and APOE differences at baseline consistent with APOE ε4 increasing the likelihood of amyloidosis[8, 33, 34] and male sex[8, 34] increasing the likelihood of neurodegeneration.

We refer to participants who underwent imaging as being drawn from a population based cohort. Still, it is reasonable to question the effect of participation bias in the subset who agreed to imaging. We note that the Table shows only minor demographic differences in the imaged sample compared to the overall sample. We also note that in a sensitivity analysis we found no difference in dementia rates among those who did vs did not participate in

imaging (see supplementary material). Thus while participation bias in imaging may exist, it does not seem to be related to the primary clinical outcome of dementia.

Supplementary Material

Refer to Web version on PubMed Central for supplementary material.

Acknowledgments

Funding

National Institute on Aging; Alexander Family Professorship of Alzheimer's Disease Research; the GHR Foundation.

This study was supported by the US National Institute on Aging, the Alexander Family Professorship of Alzheimer's Disease Research, and the GHR Foundation.

References

1. Dubois B, Feldman HH, Jacova C, Hampel H, Molinuevo JL, Blennow K, et al. Advancing research diagnostic criteria for Alzheimer's disease: the IWG-2 criteria. Lancet Neurol. 2014; 13(6):614–29. [PubMed: 24849862]
2. Albert MS, DeKosky ST, Dickson D, Dubois B, Feldman HH, Fox NC, et al. The diagnosis of mild cognitive impairment due to Alzheimer's disease: Recommendations from the National Institute on Aging and Alzheimer's Association Workgroup. Alzheimers Dement. 2011; 7(3):270–9. [PubMed: 21514249]
3. McKhann GM, Knopman DS, Chertkow H, Hyman BT, Jack CR Jr, Kawas CH, et al. The diagnosis of dementia due to Alzheimer's disease: Recommendations from the National Institute on Aging and the Alzheimer's Assocation Workgroup. Alzheimers Dement. 2011; 7(3):263–9. [PubMed: 21514250]
4. Sperling RA, Aisen PS, Beckett LA, Bennett DA, Craft S, Fagan AM, et al. Toward defining the preclinical stages of Alzheimer's disease: recommendations from the National Institute on Aging-Alzheimer's Assocation workgroups on diagnostic guidelines for Alzheimer's disease. Alzheimers Dement. 2011; 7(3):280–92. [PubMed: 21514248]
5. Villemagne VL, Fodero-Tavoletti MT, Masters CL, Rowe CC. Tau imaging: early progress and future directions. The Lancet Neurology. 2015; 14(1):114–24. [PubMed: 25496902]
6. Marquie M, Normandin MD, Vanderburg CR, Costantino IM, Bien EA, Rycyna LG, et al. Validating novel tau positron emission tomography tracer [F-18]-AV-1451 (T807) on postmortem brain tissue. Ann Neurol. 2015 Epub ahead of print.
7. Jack CR Jr, Knopman DS, Weigand SD, Wiste HJ, vemuri P, Lowe V, et al. An operational approach to NIA-AA crtiteria for preclinical Alzheimer's disease. Ann Neurol. 2012; 71(6):765–75. [PubMed: 22488240]
8. Jack CR Jr, Wiste HJ, Weigand SD, Rocca WA, Knopman DS, Mielke MM, et al. Age-specific population frequencies of cerebral beta-amyloidosis and neurodegeneration among people with normal cognitive function aged 50–89 years: a cross-sectional study. The Lancet Neurology. 2014; 13(10):997–1005. [PubMed: 25201514]
9. Roberts RO, Geda YE, Knopman DS, Cha RH, Pankratz VS, Boeve BF, et al. The Mayo Clinic Study of Aging: design and sampling, participation, baseline measures and sample characteristics. Neuroepidemiology. 2008; 30(1):58–69. [PubMed: 18259084]
10. Klunk WE, Engler H, Nordberg A, Wang Y, Blomqvist G, Holt DP, et al. Imaging brain amyloid in Alzheimer's disease with Pittsburgh Compound-B. Ann Neurol. 2004; 55(3):306–19. [PubMed: 14991808]
11. Senjem ML, Gunter JL, Shiung MM, Petersen RC, Jack CR Jr. Comparison of different methodological implementations of voxel-based morphometry in neurodegenerative disease. Neuroimage. 2005; 26(2):600–8. [PubMed: 15907317]

12. Dickerson BC, Bakkour A, Salat DH, Feczko E, Pacheco J, Greve DN, et al. The cortical signature of Alzheimer's disease: regionally specific cortical thinning relates to symptom severity in very mild to mild AD dementia and is detectable in asymptomatic amyloid-positive individuals. Cereb Cortex. 2009; 19(3):497–510. [PubMed: 18632739]
13. Jack CR, Wiste HJ, Weigand S, Knopman D, Mielke MM, Vemuri P, et al. Different definitions of neurodegeneration produce similar frequencies of amyloid and neurodegeneration biomarker groups by age among cognitively non-impaired individuals. Brain. 2015 Epub ahead of print.
14. Jack CR Jr, Petersen RC, Xu YC, Waring SC, O'Brien PC, Tangalos EG, et al. Medial temporal atrophy on MRI in normal aging and very mild Alzheimer's disease. Neurology. 1997; 49(3):786–94. [PubMed: 9305341]
15. Barnes J, Ridgway GR, Bartlett J, Henley SM, Lehmann M, Hobbs N, et al. Head size, age and gender adjustment in MRI studies: a necessary nuisance? Neuroimage. 2010; 53(4):1244–55. [PubMed: 20600995]
16. Murray ME, Lowe VJ, Graff-Radford NR, Liesinger AM, Cannon A, Przybelski SA, et al. Clinicopathologic and 11C-Pittsburgh compound B implications of Thal amyloid phase across the Alzheimer's disease spectrum. Brain. 2015; 138(Pt 5):1370–81. [PubMed: 25805643]
17. Jackson C. Multi-State Models for Panel Data: The msm Package for R. Journal of Statistical Software. 2011; 38(8):1–28.
18. St Sauver JL, Grossardt BR, Leibson CL, Yawn BP, Melton LJ, Rocca WA. Generalizability of epidemiological findings and public health decisions: an illustration from the Rochester Epidemiology Project. Mayo Clin Proc. 2012; 87(2):151–60. [PubMed: 22305027]
19. Knopman DS, Jack CR Jr, Wiste HJ, Weigand SD, Vemuri P, Lowe VJ, et al. Brain injury biomarkers are not dependent on beta-amyloid in normal elderly. Ann Neurol. 2013; 73(4):472–80. [PubMed: 23424032]
20. Nelson PT, Head E, Schmitt FA, Davis PR, Neltner JH, Jicha GA, et al. Alzheimer's disease is not "brain aging": neuropathological, genetic, and epidemiological human studies. Acta Neuropathol. 2011; 121(5):571–87. [PubMed: 21516511]
21. Schneider JA, Aggarwal NT, Barnes L, Boyle P, Bennett DA. The neuropathology of older persons with and without dementia from community versus clinic cohorts. J Alzheimers Dis. 2009; 18(3): 691–701. [PubMed: 19749406]
22. Crary JF, Trojanowski JQ, Schneider JA, Abisambra JF, Abner EL, Alafuzoff I, et al. Primary age-related tauopathy (PART): a common pathology associated with human aging. Acta Neuropathol. 2014; 128(6):755–66. [PubMed: 25348064]
23. Fjell AM, McEvoy L, Holland D, Dale AM, Walhovd KB. Brain changes in older adults at very low risk for Alzheimer's disease. J Neurosci. 2013; 33(19):8237–42. [PubMed: 23658162]
24. Jagust W. Vulnerable neural systems and the borderland of brain aging and neurodegeneration. Neuron. 2013; 77(2):219–34. [PubMed: 23352159]
25. Knopman DS, Jack CR Jr, Wiste HJ, Weigand SD, Vemuri P, Lowe VJ, et al. Selective worsening of brain injury biomarker abnormalities in cognitively normal elderly persons with beta-amyloidosis. JAMA Neurol. 2013; 70(8):1030–8. [PubMed: 23797806]
26. Nelson PT, Alafuzoff I, Bigio EH, Bouras C, Braak H, Cairns NJ, et al. Correlation of Alzheimer disease neuropathologic changes with cognitive status: a review of the literature. J Neuropathol Exp Neurol. 2012; 71(5):362–81. [PubMed: 22487856]
27. Mormino EC, Kluth JT, Madison CM, Rabinovici GD, Baker SL, Miller BL, et al. Episodic memory loss is related to hippocampal-mediated beta-amyloid deposition in elderly subjects. Brain. 2009; 132(Pt 5):1310–23. [PubMed: 19042931]
28. Jack CR Jr, Lowe VJ, Weigand SD, Wiste HJ, Senjem ML, Knopman DS, et al. Serial PIB and MRI in normal, mild cognitive impairment and Alzheimer's disease: implications for sequence of pathological events in Alzheimer's disease. Brain. 2009; 132(pt 5):1355–65. [PubMed: 19339253]
29. Bertens D, Knol DL, Scheltens P, Visser PJ. Temporal evolution of biomarkers and cognitive markers in the asymptomatic, MCI, and dementia stage of Alzheimer's disease. Alzheimers Dement. 2015; 11(5):511–22. [PubMed: 25150730]

30. Yau WY, Tudorascu DL, McDade EM, Ikonomovic S, James JA, Minhas D, et al. Longitudinal assessment of neuroimaging and clinical markers in autosomal dominant Alzheimer's disease: a prospective cohort study. The Lancet Neurology. 2015; 14(8):804–13. [PubMed: 26139022]
31. Villain N, Chetelat G, Grassiot B, Bourgeat P, Jones G, Ellis KA, et al. Regional dynamics of amyloid-beta deposition in healthy elderly, mild cognitive impairment and Alzheimer's disease: a voxelwise PiB-PET longitudinal study. Brain. 2012; 135(Pt 7):2126–39. [PubMed: 22628162]
32. Villemagne VL, Burnham S, Bourgeat P, Brown B, Ellis KA, Salvado O, et al. Amyloid beta deposition, neurodegeneration, and cognitive decline in sporadic Alzheimer's disease: a prospective cohort study. Lancet Neurol. 2013; 12(4):357–67. [PubMed: 23477989]
33. Jansen WJ, Ossenkoppele R, Knol DL, et al. Prevalence of cerebral amyloid pathology in persons without dementia: A meta-analysis. JAMA. 2015; 313(19):1924–38. [PubMed: 25988462]
34. Jack CR Jr, Wiste HJ, Weigand SD, Knopman DS, Vemuri P, Mielke MM, et al. Age, Sex, and APOE epsilon4 Effects on Memory, Brain Structure, and beta-Amyloid Across the Adult Life Span. JAMA Neurol. 2015; 72(5):511–9. [PubMed: 25775353]

Authors' contributions

Dr. Jack (Jack.Clifford@mayo.edu) conceptualization of the study, analysis and interpretation of data, drafting and revising manuscript. Dr. Jack had full access to all the data in the study and takes responsibility for the integrity of the data and the accuracy of the data analysis.

Dr. Therneau (Therneau.terry@mayo.edu) analysis and interpretation of data, drafting and revising manuscript, statistical analysis

Ms. Wiste (Wiste.Heather@mayo.edu) conceptualization of the study, analysis and interpretation of data, drafting and revising manuscript, statistical analysis

Mr. Weigand (Weigand.Stephen@mayo.edu) conceptualization of the study, analysis and interpretation of data, drafting and revising manuscript, statistical analysis

Dr. Knopman (Knopman@mayo.edu) drafting and revising manuscript

Dr. Lowe (vlowe@mayo.edu) data collection, drafting and revising the manuscript

Dr. Mielke (Mielke.Michelle@mayo.edu) drafting and revising manuscript

Dr. Vemuri (Vemuri.prashanthi@mayo.edu) drafting and revising manuscript

Dr. Roberts (Roberts.Rosebud@mayo.edu) drafting and revising manuscript

Dr. Machulda (Machulda.Mary@mayo.edu) drafting and revising the manuscript

Mr. Senjem (Senjem.matthew1@mayo.edu) analysis and interpretation of data, drafting and revising manuscript

Dr. Gunter (gunter.jeffrey@mayo.edu) analysis and interpretation of data, drafting and revising manuscript

Dr. Rocca (rocca@mayo.edu) drafting and revising manuscript

Dr. Petersen (peter8@mayo.edu) analysis and interpretation of data, drafting and revising manuscript

Declaration of interests

Dr. Jack has provided consulting services for Eli Lilly Co. He receives research funding from the National Institutes of Health ((R01 AG011378, U01 HL096917, U01 AG024904, RO1 AG041851, R01 AG037551, R01 AG043392, U01 AG006786)) and the Alexander Family Alzheimer's Disease Research Professorship of the Mayo Foundation.

Dr. Therneau receives research support from the NIH as a Co-Investigator on the following grants: R01 AG31750, R01 CA163803, R01 NR15259, R01 AG41851, R01 AR46849, R01 EB16966, P30 CA15083, R01 CA107476, R01 CA168762, R01 AR27065, R21 AG45228 and R01 HL120859.

Ms. Wiste has nothing to disclose.

Mr. Weigand has nothing to disclose.

Dr. Knopman serves as Deputy Editor for *Neurology*®; serves on a Data Safety Monitoring Board for Lundbeck Pharmaceuticals and for the DIAN study; is an investigator in clinical trials sponsored by TauRX Pharmaceuticals, Lilly Pharmaceuticals and the Alzheimer's Disease Cooperative Study; and receives research support from the NIH.

Dr. Lowe is a consultant for Bayer Schering Pharma and Piramal Imaging and receives research support from GE Healthcare, Siemens Molecular Imaging, AVID Radiopharmaceuticals, the NIH (NIA, NCI), the Elsie and Marvin Dekelboum Family Foundation, the MN Partnership for Biotechnology and Medical Genomics and the Leukemia & Lymphoma Society.

Dr. Mielke receives funding from the NIH, Driskill Foundation, Michael J. Fox Foundation, and Alzheimer's Drug Discovery Foundation outside the submitted work.

Dr. Vemuri receives funding from NIH.

Dr. Roberts receives research support from the NIH [U01 AG006786 (co-I)].

Dr. Machulda receives funding from NIH.

Mr. Senjem has nothing to disclose.

Dr. Gunter has nothing to disclose.

Dr. Rocca receives research support from the NIH [R01 AG034676 (Co-PI), U01 AG006786 (Co-I) and P50 AG044170 (Co-Director)].

Dr. Petersen serves on a data monitoring committee for Pfizer, Inc., and Janssen Alzheimer Immunotherapy and is a consultant for Merck, Incorporated, Roche, Incorporated, and Genentech, Incorporated; receives royalties from publishing *Mild Cognitive Impairment*

(Oxford University Press, 2003); and receives research support from the NIH [P50 AG16574 (PI), U01 AG06786 (PI), U01 AG24904 (Co-I) and R01 AG11378 (Co-I)].

Research in Context

Evidence before this study

We searched PubMed for reports published in English from March 2005 to October 7, 2015 with the search terms “aging and brain volume”, “amyloid PET”, “aging and amyloid PET”, and “aging and FDG PET”, “aging and brain atrophy”. We included studies in which participants underwent cross-sectional or serial biomarker tests that enabled assessment of both amyloidosis and neurodegeneration.

Added value of this study

We found no prior studies that provided estimates of rates of AD biomarker state transitions by age. We also found that studies that included serial multi-modality imaging assessment of non-demented individuals using MRI, FDG PET, and amyloid PET usually did not include a wide age range and/or involved groups of selected volunteers rather than population-based samples.

Implications of all the available evidence

Because our baseline group was non-demented, the biomarker group labels do not map onto categories currently defined by either the NIA-AA or IWG, which separate those who are cognitively normal for age from those with a mild cognitive impairment. We do not regard the composition of our baseline group as a limitation because the concept of being non-demented is familiar and meaningful to clinicians. In addition, by pooling these participants we gain numbers of transitions which are needed to power the present analysis.

Unlike age-specific frequencies, state-to-state transition rates can be thought of as direct measures of the intensity of underlying biological processes acting on an individual. The fact that transition rates of A−N− to A−N+ (SNAP); A+N− to A+N+; A−N+ (SNAP) to A+N+; A+N+ to dementia; and A−N+ to dementia all fit a simple exponential functional form with age is noteworthy (Figs 2–5). Thus, key aspects of brain aging can be conceptualized as a nearly inevitable *acceleration* toward worse biomarker and or clinical states. On a positive note, however, because these state-to-state transition rates increase exponentially with age, a small therapeutically induced reduction in these transition rates from a less- to a more-abnormal state in middle age can be expected to result in important reductions in population frequencies of worse states at later ages.

Assuming a cohort of non-demented A−N− individuals at age 50, by age 90, 73% would be deceased, and 79% would be deceased or demented (Fig 6a). Therefore, when interpreting biomarker modeling data in very old non-demented participants, it is important to bear in mind that these participants represent only a small fraction of their age cohort. Participants who are alive and non-demented beyond age 85 or so are well outside the norm for their age cohort, and represent highly successful aging.

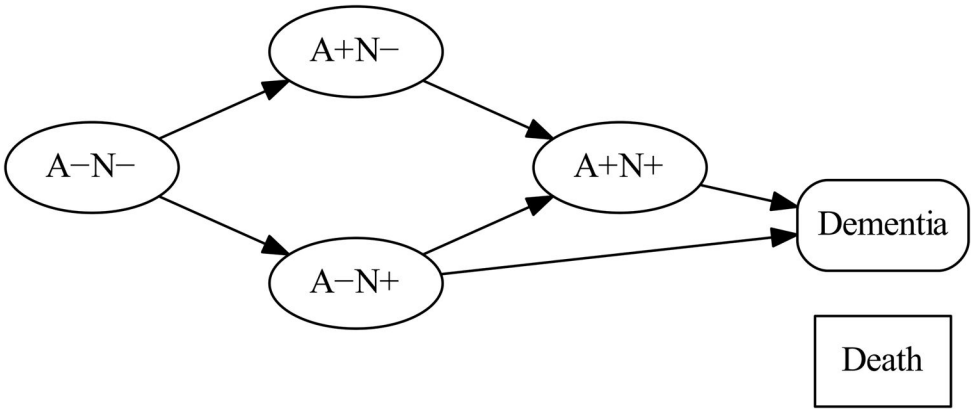

Figure 1. Diagram of the multi-state transition model

Each node denotes one of the six states in the model. Node shapes denote the type of state. Ovals represent the four different A/N biomarker states among non-demented participants. The rounded box represents dementia. The rectangular box represents death. The six arrows represent the six forward transition rates between states that were estimated in our model. All states were allowed to transition to death in the model; however, for the sake of readability we do not show the arrows corresponding to transitions to death. Our model allowed each transition rate to vary by age and so we estimated the transition rate corresponding to each arrow for a specified age. While theoretically subjects should only move from less abnormal to more abnormal states, in reality, some “backward” transitions were observed in our data. These backward transitions were rare and likely due to misclassification, but to accommodate them, the model included a single estimated transition rate from a more abnormal to a less abnormal biomarker state (0.025) that did not vary by age (arrows not shown).

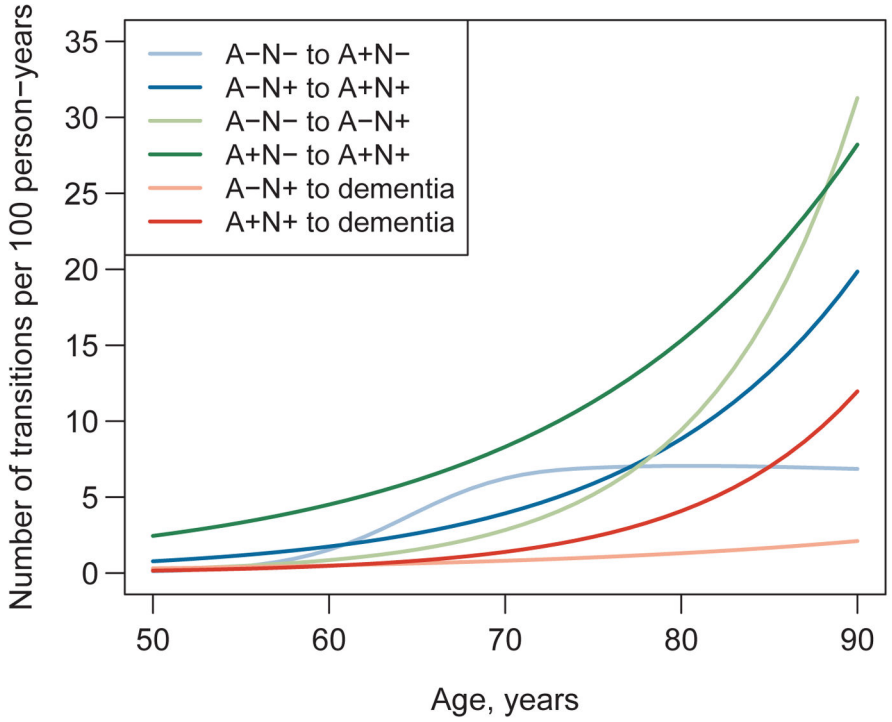

Figure 2. Estimated biomarker transition rates by age

The A−N− to A+N− transition rate was allowed to vary non-linearly on the log scale with age by modeling it with restricted cubic splines with knot as ages 55, 65, 75, and 90. All other transitions were modeled with linear (on the log-scale) age effects. Blue shades indicate transitions from A− to A+. Green shades indicate transitions from N− to N+. Red shades indicate transitions to dementia.

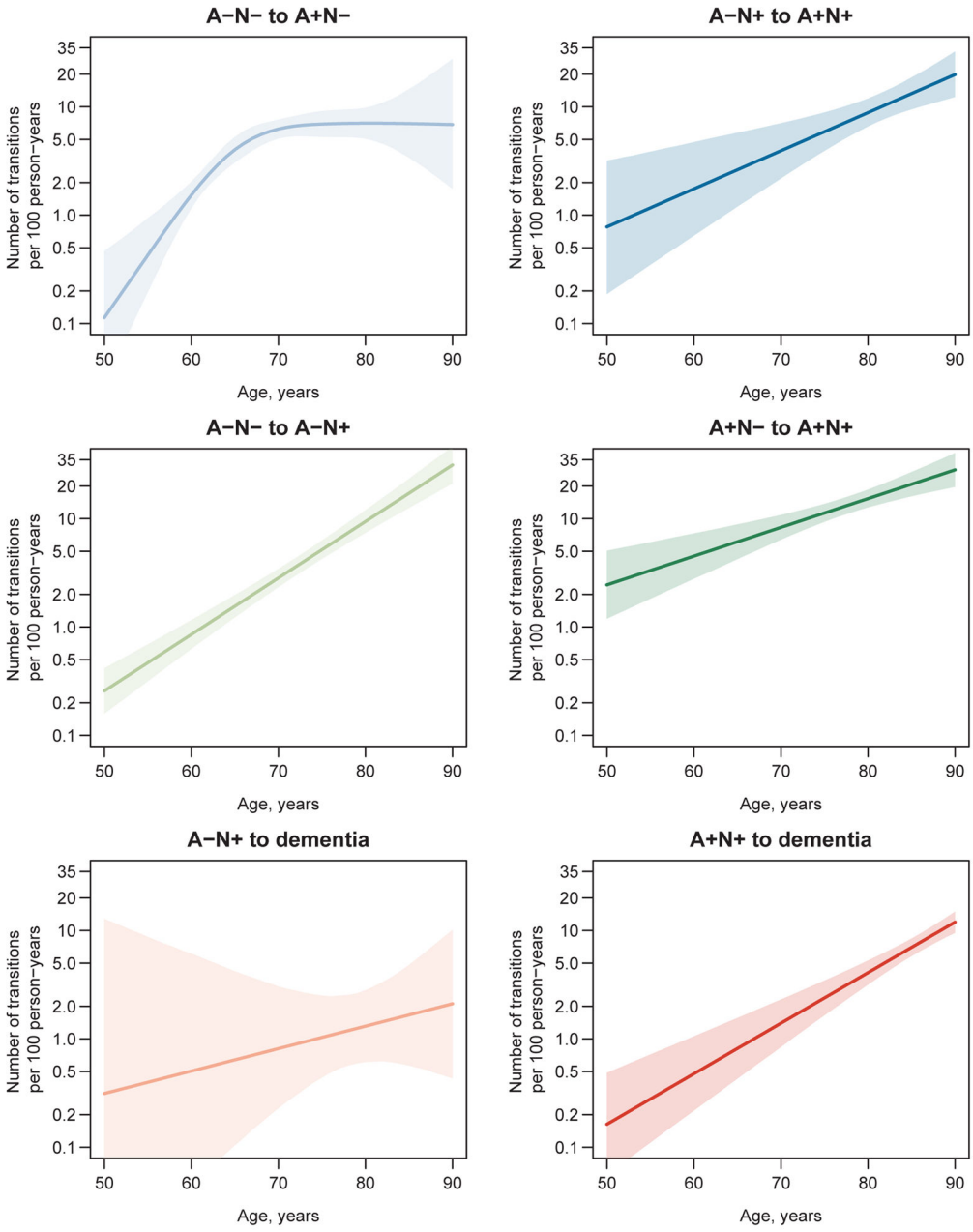

Figure 3. Confidence intervals for estimated biomarker transition rates plotted on log scale

Note the difference in the scale between Fig 2 (arithmetic scale) and Fig 3 (log scale). The data in Fig 3 are plotted on log scale to demonstrate variance around the regression line for each rate in terms of coefficient of variation. Shaded areas indicate 95% pointwise confidence intervals. Confidence intervals were obtained by first randomly generating 10,000 multivariate normal variates centered at the maximum likelihood estimates with the variance-covariance matrix equal to the inverse of the negative of the Hessian matrix. Age-specific rates were calculated for each of the 10,000 variates and the 95% pointwise CIs were calculated as the 2.5th and 97.5th quantiles of these simulated age-specific rates.

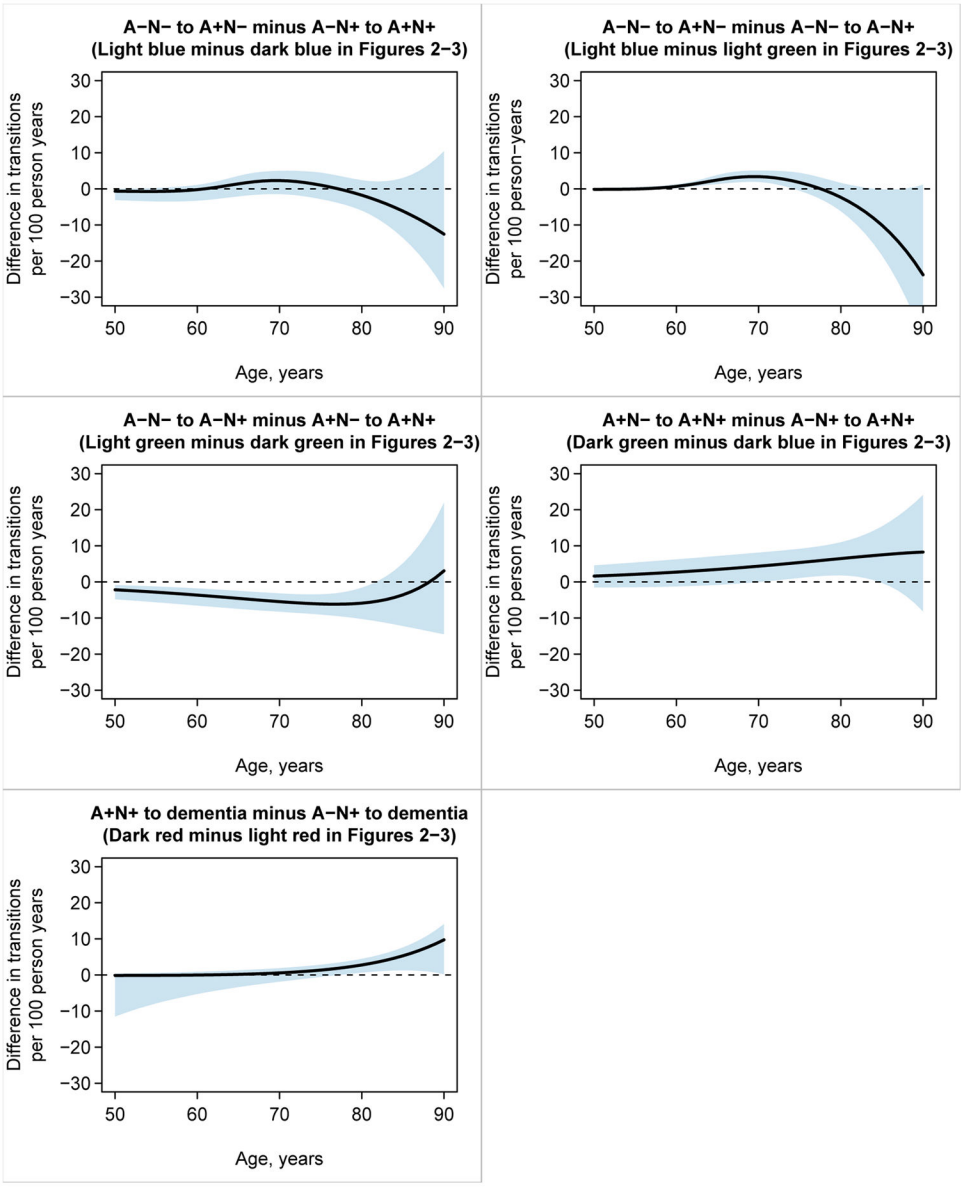

Figure 4. Estimates and 95% confidence intervals for differences between transition rates for selected transitions

We interpret 95% CIs that do not include the null value of zero as significantly different at $p<0.05$. Confidence intervals for the difference in rates were obtained as described for Figure 3 except that the 2.5^{th} and 97.5^{th} quantiles were calculated not from the distribution of simulated rates but from the distribution of the difference in simulated rates (i.e., the 2.5^{th} and 97.5^{th} quantiles of the 10,000 simulated rate differences at each age).

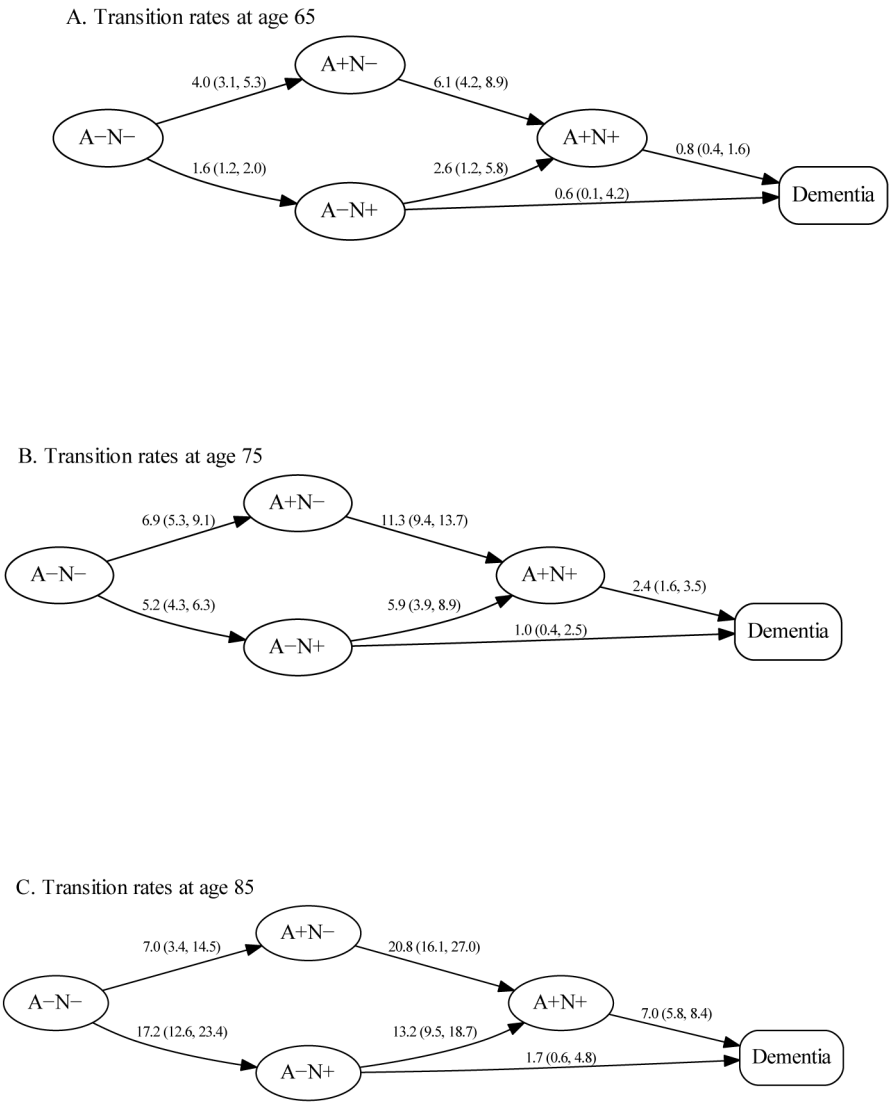

Figure 5. Transition rates among the four biomarker states within non-demented participants and to dementia at ages 65, 75, and 85 years

Rates are expressed as number of transitions per 100 person-years (95% CI).

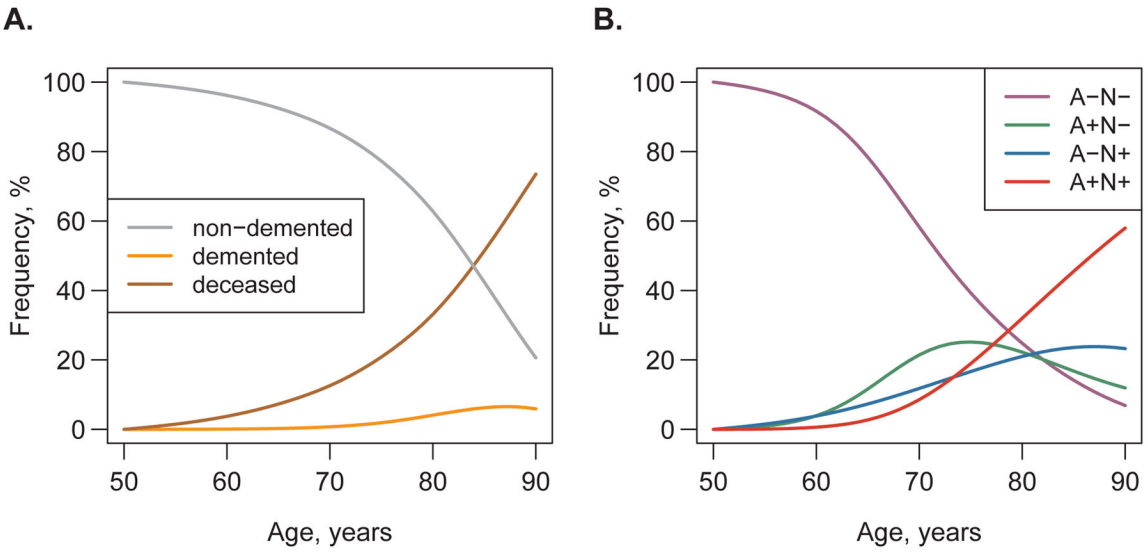

Figure 6. Estimated frequency of states by age

Assuming a cohort of non-demented A−N− participants aged 50, we used the transition rates to estimate what the frequency of each state will be as these participants age from 50 to 90. Panel A shows the estimated frequency of non-demented (cognitively normal for age and MCI) participants, participants with dementia, and participants who have died by age. Panel B shows the estimated frequency of participants in each of the four biomarker groups by age among those participants who remain alive and non-demented.

Table 1

Baseline characteristics of study participants overall and by biomarker status at the first imaging visit

Characteristic	All MCSA n=4049	Imaged MCSA n=1541	A−N− n=778	A+N− n=247	A−N+ n=233	A+N+ n=283
Clinical diagnosis, n (%)						
CN	3512 (87%)	1355 (88%)	739 (95%)	222 (90%)	197 (85%)	197 (70%)
MCI	537 (13%)	186 (12%)	39 (5%)	25 (10%)	36 (15%)	86 (30%)
Age, years, median (IQR)	75 (69, 81)	72 (64, 79)	66 (60, 73)	74 (69, 79)	77 (72, 83)	81 (77, 85)
Male gender, n (%)	2060 (51%)	819 (53%)	409 (53%)	111 (45%)	145 (62%)	154 (54%)
APOE ε4 positive, n (%)	1091 (28%)	428 (29%)	157 (21%)	109 (44%)	43 (19%)	119 (42%)
Education, years, median (IQR)	14 (12, 16)	14 (12, 16)	15 (13, 17)	14 (12, 16)	14 (12, 16)	14 (12, 16)
MMSE score, median (IQR)	28 (27, 29)	29 (27, 29)	29 (28, 29)	29 (27, 29)	28 (27, 29)	28 (27, 29)
Amyloid PET, SUVR						
Median (IQR)		1.34 (1.28, 1.49)	1.29 (1.25, 1.33)	1.60 (1.46, 1.91)	1.32 (1.28, 1.35)	1.81 (1.50, 2.24)
> 1.40, n (%)*		530 (34%)	0 (0%)	247 (100%)	0 (0%)	283 (100%)
FDG PET, SUVR						
Median (IQR)		1.46 (1.35, 1.57)	1.53 (1.45, 1.62)	1.46 (1.40, 1.55)	1.31 (1.25, 1.44)	1.28 (1.21, 1.37)
< 1.32, n (%)*		333 (22%)	0 (0%)	0 (0%)	142 (61%)	191 (67%)
AD signature thickness, mm						
Median (IQR)		2.88 (2.76, 2.98)	2.95 (2.86, 3.03)	2.90 (2.83, 2.98)	2.72 (2.64, 2.81)	2.68 (2.57, 2.78)
< 2.74, n (%)*		341 (22%)	0 (0%)	0 (0%)	141 (61%)	200 (71%)
Subjects with follow-up, n (%)	3840 (95%)	1158 (75%)	510 (66%)	199 (81%)	203 (87%)	246 (87%)
Years of follow-up, Median (IQR)†	4.0 (2.1, 7.0)	2.6 (1.2, 3.9)	2.1 (1.1, 3.8)	2.6 (1.2, 4.0)	3.7 (2.4, 4.6)	3.6 (2.3, 4.1)
Subjects with serial imaging, n (%)		489 (32%)	190 (24%)	89 (36%)	96 (41%)	114 (40%)
Years of imaging follow-up, Median (IQR)‡		2.6 (1.6, 3.9)	2.5 (2.2, 3.9)	2.7 (1.4, 3.9)	2.7 (1.4, 3.9)	2.6 (1.4, 3.8)

*Number (%) of subjects classified as abnormal on the imaging measure of interest by group

†Years of follow-up are shown among subjects calculated as time from baseline visit to last follow-up and among the imaging subset from first imaging visit to last follow-up. Note that some imaging subjects also had visits prior to the first imaging visit which are not summarized in the table but were included in the model.

‡Years of imaging follow-up shown among subjects with serial imaging data